Low Temperature Physics ARTICLE pubs.aip.org/aip/ltp

Magnetic and magnetoelastic properties of antiferromagnet $FeGe_2$

Cite as: Fiz. Nizk. Temp. **49**, 1129–1134 (September 2023); doi: 10.1063/10.0020594
Submitted: 25 July 2023

G. E. Grechnev, A. A. Lyogenkaya, V. A. Desnenko, A. V. Fedorchenko, and A. S. Panfilov[a)]

AFFILIATIONS

B. Verkin Institute for Low Temperature Physics and Engineering of the National Academy of Sciences of Ukraine, Kharkiv 61103, Ukraine

[a)]**Author to whom correspondence should be addressed:** panfilov@ilt.kharkov.ua

ABSTRACT

The magnetic susceptibility χ of single-crystal antiferromagnet $FeGe_2$ ($T_N = 289$ K) was measured in the temperature range from 4.2 to 300 K in a magnetic field H up to 40 kOe applied along the main crystallographic axes. For the antiferromagnetic (AFM) state at low temperatures, a strong increase in χ is observed with increasing H applied along the [100] axis, which reaches saturation at $H \geq H_0 \sim 11$ kOe. It is assumed that this behavior is associated with a field-induced change in the AFM domain structure, and the single-domain state is realized in a field above H_0 with the AFM axis perpendicular to the field direction. The study of χ under the uniaxial P_a and uniform P pressures in a wide temperature range has revealed an anomalously large increase in χ in AFM state with increasing uniaxial pressure for $P_a||H||[100]$ at $H \ll H_0$. The observed growth of χ saturates at pressure $P_a \geq P_a^* \simeq 1.5$ kbar and suggests the formation of the single-domain state for the above conditions. The values of uniform pressure effect on χ was found to lie in the range $d\ln\chi/dP = -(2\text{–}3)$ Mbar^{-1}, being weakly dependent on the magnetic state and field direction. In addition, the uniform pressure effect on the transition temperature between two AFM structures in $FeGe_2$, $T_M \simeq 263$ K, was found to be weak.

1. INTRODUCTION

Transition metal compounds with germanium exhibit unusual magnetic, electrical and structural properties. These properties make them the subject of continuous experimental and theoretical investigations (see Ref. 1 and references therein). A typical representative of these materials is the Fe-Ge system, in which the variety of properties depends on the composition.[2] In this work, we studied the features of magnetism of the $FeGe_2$ compound, the structural modification of which in the form of nanowires[3] and a metastable layered polymorph of $FeGe_2$[4] are promising materials for spintronics.

Itinerant antiferromagnet $FeGe_2$ crystallizes with the body-centered tetragonal $CuAl_2$-type crystal structure ($a = 5.908$Å, $c = 4.955$Å), in which iron atom layers alternate with germanium atom layers.[5] According to more detailed studies of the magnetic structure of $FeGe_2$,[5–8] with decreasing temperature this compound undergoes two magnetic phase transitions, one at $T_N \simeq 289$ K from the paramagnetic phase to AFM incommensurate spin density wave state and the second at $T_M \simeq 263$ K from incommensurate to commensurate, collinear AFM structure with magnetic moments of iron atoms lying in the basal plane.

The presence of two equivalent AFM axes in $FeGe_2$, which are parallel to the crystallographic axes [100] and [010], and the existence of AFM domains determine a number of features of its magnetic properties. One of them is a strong field dependence of magnetic susceptibility of AFM phase at H applied along the [100] or [010] axis.[9,10] The specificity of this dependence is the increase in susceptibility with increasing field, in contrast to decreasing field dependence associated usually with the presence of magnetic impurities in the material. It is assumed that such behavior in $FeGe_2$ is associated with the rearrangement of the AFM domain structure in a magnetic field, namely, with an increase in the fraction of energetically more favorable domain,[9,10] which is saturated when domain rearrangement has been completed at the characteristic field $H_0 \simeq 10$–13 kOe.

Another magnetic peculiarity of $FeGe_2$ is an anomalous behavior of its magnetostriction data.[11] The measured at $T = 4.2$ K longitudinal $\varepsilon_{\parallel}(H)$ and transverse $\varepsilon_{\perp}(H)$ magnetostrictions of $FeGe_2$ in the basal plane for $H||[100]$, being approximately quadratic in the field up to $H_0 \sim 13$ kOe and similar but opposite in sign, at higher H are saturated at an anomalously large magnitude, $\varepsilon_0 \sim \pm 7 \cdot 10^{-6}$. In addition, the low field magnetostriction data[11]

indirectly indicate the giant influence of uniaxial pressure on magnetic susceptibility of the AFM phase at $H||[100]$, which motivates direct measurement of this effect.

The aim of this work is to shed more light on the parameters of domain structure in $FeGe_2$ and its evolution under magnetic field and uniaxial pressure by experimental study of magnetic susceptibility of $FeGe_2$ in a wide range of temperatures and magnetic fields together with application of uniaxial and hydrostatic pressures.

2. EXPERIMENTAL DETAILS AND RESULTS

2.1. Magnetic properties at ambient pressure

The single crystalline samples of $FeGe_2$ were spark cut from the same ingot that was used earlier in Refs. 11 and 12. The samples were in the form of rectangular parallelepipeds, having dimensions of approximately $2.5 \times 2.5 \times 5\,mm^3$ and orientations of the main crystallographic axes along the edges. The temperature and field dependencies of the magnetic susceptibility χ were measured between 4.2 and 300 K in the magnetic field H up to 40 kOe using a homemade SQUID magnetometer. The main experimental results are shown in Figs. 1–4. As can be seen in Fig. 1, which shows the dependencies of $\chi = M/H$ on the magnetic field applied along the main crystallographic axes at $T = 4.2$ K, there is an essential peculiarity of the $\chi(H)$ dependence at $H||[100]$. In this case, it was observed a strong growth of χ with increasing field up to $H_0 \sim 11$ kOe, where magnitude of χ approximately doubles and

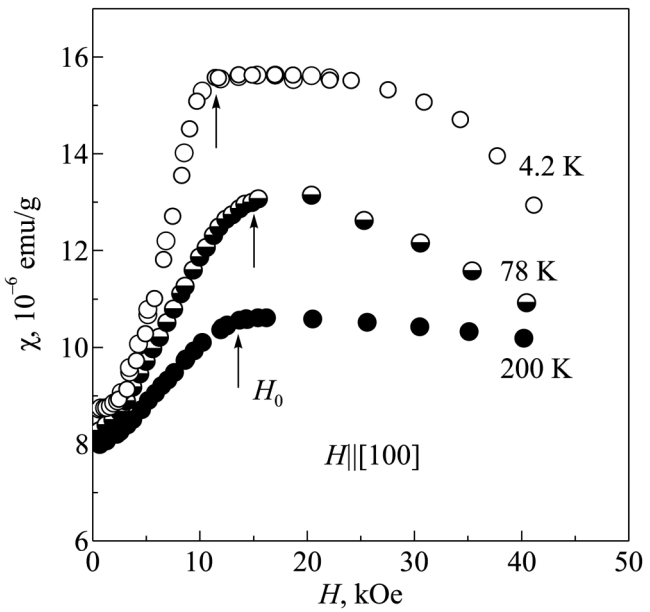

FIG. 2. Dependences of magnetic susceptibility in $FeGe_2$ on H applied along [100] axis for different temperatures. The arrows mark the value H_0 (see text for details).

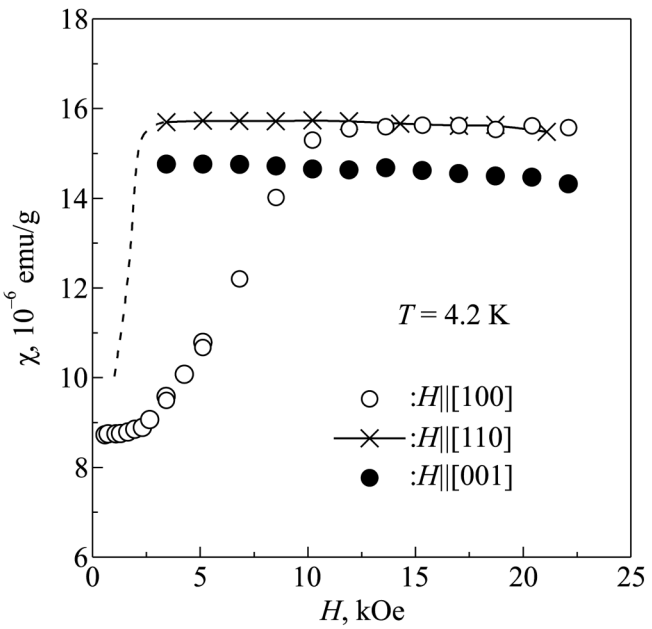

FIG. 1. Field dependences of magnetic susceptibility of $FeGe_2$ at $T = 4.2$ K for H applied along different crystal axes. The dashed line schematically marks the expected low field behavior of the $\chi(H)$ dependence for $H||[110]$ based on the experimental data in Fig. 1 of Ref. 13.

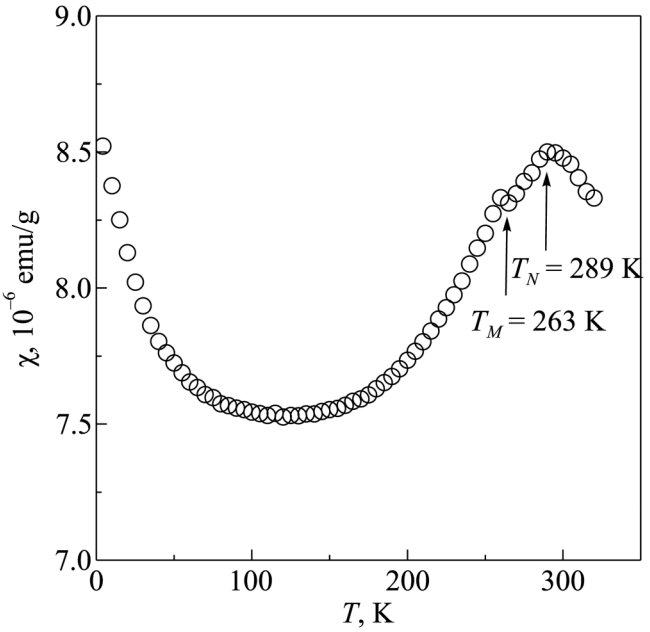

FIG. 3. Temperature dependence of magnetic susceptibility of $FeGe_2$ in the magnetic field $H = 0.2$ kOe applied along the [100] axis. The arrows mark the Néel temperature T_N and the transition temperature T_M between different AFM magnetic structures.

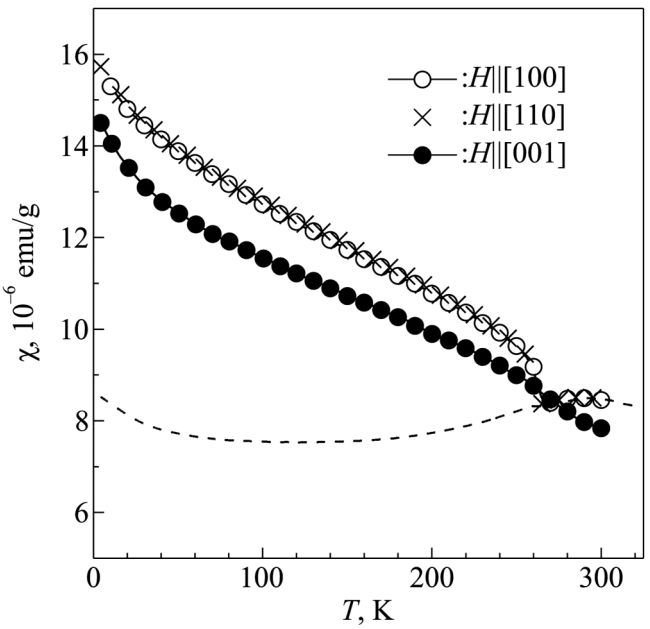

FIG. 4. Temperature dependences of magnetic susceptibility of $FeGe_2$ in the magnetic field $H = 20$ kOe applied along the main crystal axes. Dashed line shows the experimental data in low magnetic field (0.2 kOe) applied along the [100] axis.

saturates at $H \geq H_0$. The value of H_0 and the trends of its changes with temperature in the range 4–250 K (see Fig. 2) are consistent with available literature data.[10] Some decrease in susceptibility with increasing field above H_0 is apparently due to the band nature of magnetism in $FeGe_2$, namely, the manifestation of the fine structure of the AFM density of states near the Fermi level[8] and its modification by spin splitting of energy bands in a strong magnetic field, in addition to their splitting by the exchange interaction.

We also note the less studied analogous behavior of $\chi(H)$ at $H||[110]$, which is also characterized by an increase in $\chi(H)$ with increasing field and its saturation in a field $H \geq H^* \sim 2$ kOe (see Fig. 1). It is assumed that both of these features are due to the rearrangement of the domain structure of $FeGe_2$ under the action of the field which is discussed below.

The temperature dependence of magnetic susceptibility for $FeGe_2$ in magnetic field $H = 0.2$ kOe ($\ll H_0$) applied along the [100] axis is shown in Fig. 3. It exhibits maximum at $T_N = 289$ K and distinct peculiarity at the temperature of transition between different AFM structure, $T_M \simeq 263$ K.

Figure 4 shows the temperature dependence of magnetic susceptibility of $FeGe_2$ in the magnetic field $H = 20$ kOe applied along the main crystallographic axes and low field data for $H = 0.2$ kOe applied along the [100] axis (dashed line). As can be seen, the high field ($H > H_0$) data exhibit relatively weak anisotropy of susceptibility for the H directions in the basal plane and along the tetragonal axis in contrast to the low field ($H \ll H_0$) data (note that values of magnetic susceptibility for H applied along the [110] and [001] axes are practically independent on the field, see Fig. 1).

2.2. Pressure effects on magnetic properties

For study of the uniaxial pressure effect on magnetic susceptibility, the SQUID magnetometer was supplemented by a Cu-Be miniature piston-cylinder cell, which enables to produce a continuously adjustable uniaxial pressure P_a up to 1.5 kbar (see for details Ref. 14). To assure the proper P_a uniformity, the thin (~0.05 mm) teflon plates were inserted between the pistons and the sample. The magnitude of P_a was determined by a tensometric sensor. The typical dependence $\chi(P_a)$ of $FeGe_2$ in AFM state at $H = 0.2$ kOe applied as well as P_a along the [100] axis is shown in Fig. 5. It exhibits a strong increase in χ with increasing P_a, which saturates at $P_a = P_a^* \sim 1.5$ kbar reaching the high field its value. As can be seen in Fig. 6, the value of initial pressure derivative of susceptibility, $d \ln \chi(T)/dP_a$, decreases gradually with increasing temperature up to T_N.

The uniform pressure effect on the magnetic susceptibility was measured under helium gas pressure up to 2 kbar at two fixed temperatures, 78 and 300 K, using a pendulum-type magnetometer placed into the nonmagnetic pressure cell.[15] The relative errors of our measurements, performed in the magnetic field $H = 17$ kOe, did not exceed 0.05%. As can be seen in Fig. 7, the experimental dependencies $\chi(P)$ turn out to be linear within the limits of measurement errors and the range of pressures used. The corresponding values of pressure derivative of χ, $d \ln \chi/dP$, are given in Table I, exhibiting a moderate value of the pressure effect which only weakly depends on magnetic field directions and magnetic state of the sample.

In addition, the uniform pressure effect on the transition temperature between different AFM structures in $FeGe_2$, $T_M \simeq 263$ K, was measured to be weak $dT_M/dP = (0.1 \pm 0.1)$ K/kbar (Fig. 8).

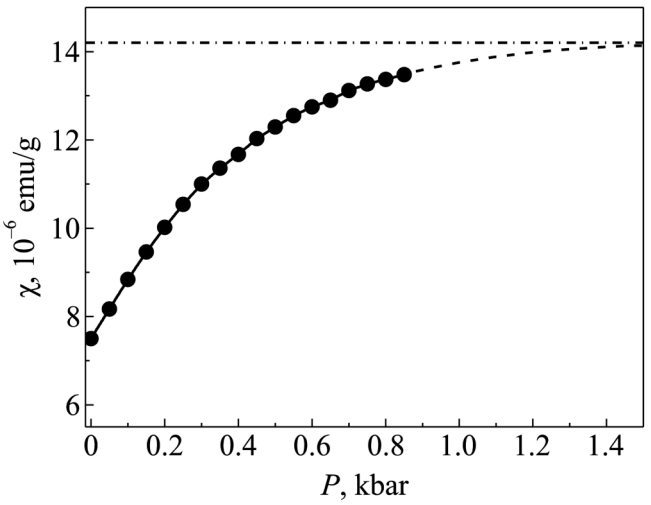

FIG. 5. The low field ($H_0 \gg H = 0.2$ kOe) magnetic susceptibility of $FeGe_2$ at $T = 45$ K as a function of the uniaxial pressure P_a. The dash-dot line denotes the high field ($H_0 < H = 20.4$ kOe) susceptibility level at ambient pressure and the same temperature. Both the magnetic field and uniaxial pressure are applied along the [100] axis.

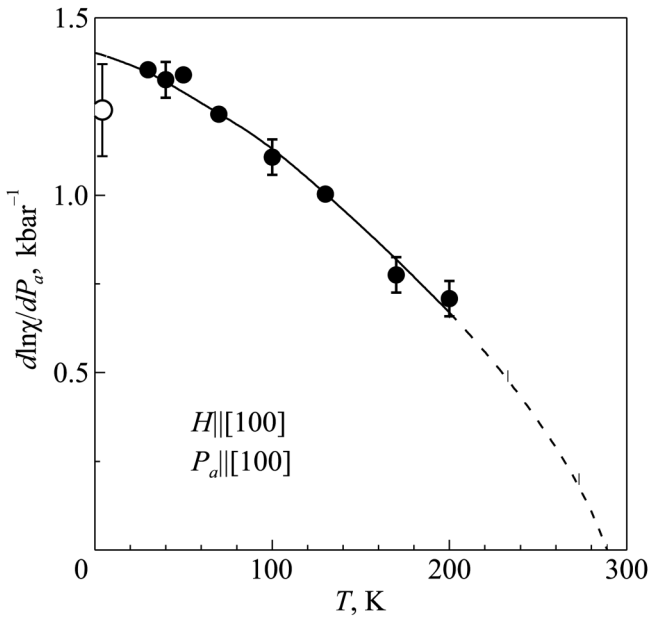

FIG. 6. Initial pressure derivative of magnetic susceptibility of $FeGe_2$ as a function of temperature for uniaxial stress P_a and magnetic field $H = 0.2$ kOe both applied along the [100] axis. The circle symbol (○) marks the value based on magnetostriction data,[11] see text for details.

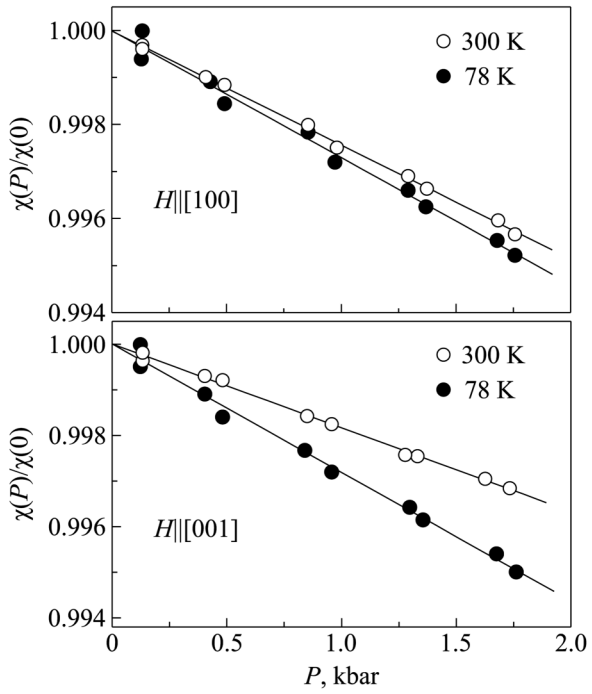

FIG. 7. Pressure dependences of magnetic susceptibility of $FeGe_2$ at $T = 78$ and 300 K for different directions of the applied magnetic field $H = 17$ kOe.

TABLE I. The magnetic susceptibility and its pressure derivative in $FeGe_2$ at $T = 78$ and 300 K for magnetic field applied along [100] and [001] axes .

Direction of the magnetic field	χ, 10^{-6} emu/g		$d\ln\chi/dP$, $Mbar^{-1}$	
	78 K	300 K	78 K	300 K
$H\|\|$ [100]	13.98	8.85	-2.7 ± 0.3	-2.4 ± 0.2
$H\|\|$ [001]	12.44	8.17	-2.8 ± 0.3	-1.9 ± 0.2

3. DISCUSSION

As noted earlier, the $FeGe_2$ compound has two equivalent AFM axes, which favors the formation of a two-domains AFM structure that determines the features of its magnetic properties. Thus, when a magnetic field is applied, for example, in the basal plane, the domains with assumed AFM axes parallel to [100] or [010] crystallographic axes turn out to be energy non-equivalent (except for the case of $H||[110]$). The applied field exerts a pressure on interdomain walls and causes their displacement.[9,10] In the case of $H||[100]$, the magnetic susceptibility, $\chi(T, H) = M(T, H)/H$, is the sum of contribution of each domain,

$$\chi(T, H) = \frac{M(T, H)}{H} = c_1(H)\chi_{\|}(T) + c_2(H)\chi_{\perp}(T), \qquad (1)$$

where c_i is a fractional content of ith domain and $\chi_{\|}$ and $\chi_{\perp}$ are the temperature dependent mass magnetic susceptibilities of domains with AFM axes being parallel and perpendicular to applied field,

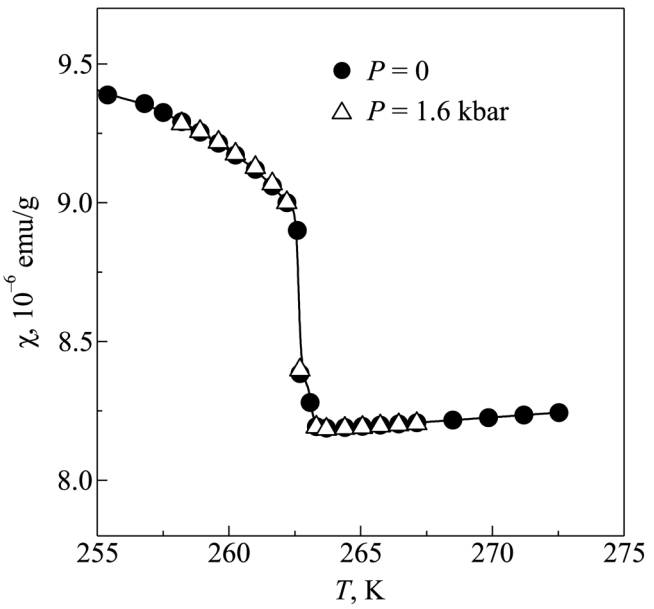

FIG. 8. Temperature dependences of magnetic susceptibility of $FeGe_2$ around $T_M(\simeq 263$ K) in magnetic field $H = 17$ kOe applied along [100] axis for two different pressures. The higher pressure data are shifted upwards to about $0.03 \cdot 10^{-6}$ emu/g for convenience of comparison.

respectively. Using our experimental data on $\chi(T, H)$ allowed to evaluate $\chi_{\parallel}(T)$ and $\chi_{\perp}(T)$ (see Fig. 9), assuming these characteristics to be nearly independent of the field. As $\chi_{\perp}(T)$ it was reasonable to take the high field values of $\chi_{100}(T)$ in Fig. 4, accepting in Eq. (1) $c_1 = 0$ and $c_2 = 1$. Then $\chi_{\parallel}(T)$ was determined by subtracting the estimated value of $\chi_{\perp}(T)$ from the sum of $\chi_{\parallel}(T)$ and $\chi_{\perp}(T)$ at low field (dashed line in Fig. 4), taking in Eq. (1) the initial fractional content of both domains to be equal $c_1 = c_2 = 0.5$. Thus, the approach presented here implies the presence in $FeGe_2$ of two types of domains with AFM axes along the [100] and [010] directions. Their mass magnetic characteristics shown in Fig. 9 are in agreement with data of Ref. 10 but being determined in a wider temperature range. In principle, they allow to determine the magnetic moment for an arbitrary direction of the magnetic field in the basal plane provided that the fractional content of domains is known and the rotation mechanism of AFM axes is missing. In particular, for $H||[110]$, such description is not suitable, as it leads to an incorrect estimate of $\chi_{110}(T) \approx (1/2)\chi_{\perp}$ at $T = 0$ K. The rotation mechanism must then be turned on, giving $\chi_{110}(T) = \chi_{\perp}(T)$.[9,10] In this case, the above value of field $H^* \sim 2$ kOe corresponds to the completion of the spin reorientation, when the AFM axes of both domains become perpendicular to the applied magnetic field, realizing the quasi-single-domain state.

Let's now discuss the magnetoelastic properties and start by reviewing the literature magnetostriction data for $FeGe_2$[11] and our results on uniaxial pressure effect.

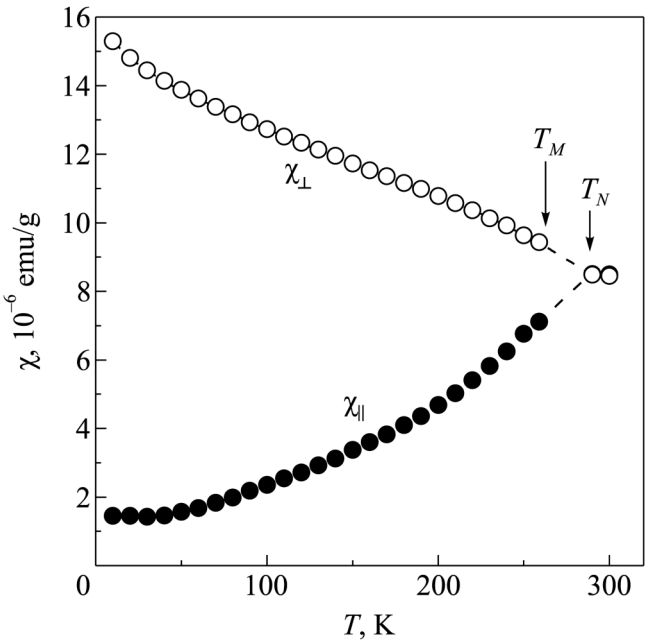

FIG. 9. Temperature dependences of the mass magnetic susceptibility in $H||[100]$ for domains with AFM axis parallel to the applied field $\chi_{\parallel}$ and perpendicular to the field $\chi_{\perp}$. The arrows mark the Néel temperature T_N and the temperature T_M of transition between different AFM structures.

For magnetic field applied in the a direction, the longitudinal magnetostriction of a crystal, $\varepsilon_a = \Delta L_a/L_a$, is related thermodynamically to the uniaxial pressure derivative of the molar magnetization $\partial M_a/dP_a$,[16]

$$\frac{\partial \varepsilon_a}{\partial H_a} = -\frac{1}{\Omega}\frac{\partial M_i}{\partial P_a}, \tag{2}$$

where Ω is the molar volume, L_a is the corresponding length of the sample. Assuming in Eq. (2) $M_a = \chi_a H_a$, where χ_a molar susceptibility, one obtains

$$\frac{\partial \varepsilon_a}{\partial H_a} = -\frac{1}{\Omega}\frac{\partial \chi_a}{\partial P_a} H_a, \tag{3}$$

which gives on integration

$$\frac{\partial \chi_a}{\partial P_a} = -\frac{\Delta L_a}{L_a}\frac{2\Omega}{H_a^2}. \tag{4}$$

For $FeGe_2$, the available experimental data at $T = 4.2$ K[11] show that, in particular, the longitudinal magnetostriction in field applied along the [100] axis is roughly quadratic at low fields ($H < H_0 \simeq 13$ kOe), being saturated at $H \geq H_0$, at the value $\Delta L_{100}/L_{100} \simeq -7 \cdot 10^{-6}$. Substituting the latter value together with values of $H_0 = 13$ kOe and $\Omega = 26.3$ cm^3 in Eq. (4) gives at $T = 4.2$ K a rough estimate

$$\frac{\partial \chi_{100}}{\partial P_{100}} \simeq 11 \cdot 10^{-6}(\text{emu/g}) \cdot \text{kbar}^{-1}. \tag{5}$$

Normalized to the low field value of $\chi_{100} = 8.5 \cdot 10^{-6}$ emu/g at $T = 4.2$ K, the obtained result corresponds to $\partial \ln \chi_{100}/\partial P_{100} \simeq 1.3$ kbar^{-1} which is consistent with our directly measured data shown in Fig. 6 confirming the reliability of our measurements.

As can be seen in Fig. 5, at fixed T and low field $H||[100]$, the rate of the growth in $\chi_{100}(P_a, T)$ with increasing pressure $P_a||[100]$ decreases gradually and vanishes at $P_a^* \sim 1.5$ kbar when susceptibility reaches the value of $\chi_{100}(T)$ at the same temperature and ambient pressure but in the high field $H \geq H_0$. The observed effect is suggested to be due to alteration of the domain structure under a uniaxial pressure (similar to action of a magnetic field), which is completed at $P_a \geq P_a^* \simeq 1.5$ kbar. The final domain state is understood as the single domain structure induced by the uniaxial pressure at low magnetic field $H \ll H_0$ applied along the [100] with AFM axes being perpendicular to H. In addition, it should be noted that from the longitudinal magnetostriction data in a field along the [100] axis the single-domain phase in $FeGe_2$ is compressed along the field direction and application of the uniaxial pressure in this direction favors the formation of this phase.

4. CONCLUSION

In this paper, magnetic susceptibility of the single crystalline sample of $FeGe_2$ was measured in the temperature range 4.2–300 K in magnetic field up to 40 kOe applied along the main crystallographic axes. The obtained results suggest a field induced change in

the two-domain AFM structure and realization of a single-domain state above $H_0 \simeq 11$ kOe applied along the [100] or [010] crystallographic axis. The determined magnitudes of H_0 and specific magnetic characteristics of domains, $\chi_{\parallel}(T)$ and $\chi_{\perp}(T)$, are in reasonable agreement with the available literature data refining their values of susceptibilities at low temperature range. Magnetization along the [110] direction in the basal plane is mainly determined by AFM axes rotation while the magnetization along [100] or [010] AFM axes is basically related to displacement of the domain walls.

An anomalously large effect of the uniaxial pressure P_a on the magnetic susceptibility was observed for $FeGe_2$ in the AFM state under the conditions $P_a||H||[100]$ at $H \ll H_0$. The observed increase in χ disappears at a pressure of $P_a \geq P_a^* \simeq 1.5$ kbar and is understood as a direct manifestation of the displacement of the domain walls for the above conditions. For this case, the formation of a single-domain state under pressure is determined by a new critical parameter $P_c^* \simeq 1.5$ kbar, similar to H_0.

The values of uniform pressure effect on χ was found to lie in the range $d\ln\chi/dP = -(2\text{–}3)$ Mbar^{-1}, being weakly dependent on the magnetic state and field direction. Its value is typical for itinerant magnets. In addition, the uniform pressure effect on the transition temperature T_M appeared to be weak, $dT_M/dP = (0.1 \pm 0.1)$ K/kbar, which is approximately an order of magnitude lower than the effect of pressure on T_N, $dT_N/dP \simeq -2.8$ K/kbar, estimated in Ref. 12. This indicates a lower pressure sensitivity of the magnetic transition at T_M compared to the transition at T_N.

The authors thank V. Pluzhnikov for providing the sample of $FeGe_2$.

REFERENCES

[1]R. W. Weiss, *Compounds of Germanium, Tin and Lead. Including Biological Activity and Commercial Application* (Springer-Verlag, Berlin, Heidelberg, New York, 1973).
[2]A. Kukolova, M. Dimitrievska, A. P. Litvinchuk, S. P. Ramanandan, N. Tappy, H. Menon, M. Borg, D. Grundler, and A. Fontcuberta i Morral, Cryst. Eng. Comm. **23**, 6506 (2021).
[3]S. Tang, I. Kravchenko, T. Z. Ward, Q. Zou, J. Yi, C. Ma, M. Chi, G. Cao, A.-P. Li, D. Mandrus, and Z. Gai, Sci. Rep. **7**, 7126 (2017).
[4]Dietmar Czubak, Ph.D. dissertation, (Humboldt-Universität zu Berlin, 2022).
[5]L. M. Corliss, J. M. Hastings, W. Kunnmann, R. Thomas, J. Zhuang, R. Butera, and D. Mukamel, Phys. Rev. B **31**, 4337 (1985).
[6]A. Z. Menshikov, Yu. A. Dorofeev, G. L. Budrina, and V. M. Syromyatnikov, J. Magn. Magn. Mater. **73**, 211 (1988).
[7]C. P. Adams, T. E. Mason, S. A. M. Mentink, and E. Fawcett, J. Phys.: Condens. Matter **9**, 1347 (1997).
[8]G. E. Grechnev, J. Kübler, and I. V. Svechkarev, J. Phys.: Condens. Matter **3**, 7199 (1991).
[9]K. B. Vlasov, R. I. Zainullina, M. A. Milyaev, and V. V. Ustinov, J. Magn. Magn. Mater. **146**, 305 (1995).
[10]K. B. Vlasov, R. I. Zainullina, and M. A. Milyaev, Zh. Eksp. Teor. Fiz. **99**, 300 (1991) [Sov. Phys. JETP **72**, 169 (1991)].
[11]E. Franus-Muir, E. Fawcett, and V. Pluzhnikov, Solid State Commun. **52**, 615 (1984).
[12]V. Pluzhnikov, D. Feder, and E. Fawcett, J. Magn. Magn. Mater. **27**, 343 (1982).
[13]K. B. Vlasov, R. I. Zainullina, N. G. Bebenin, and I. I. Piratinskaya, Fiz. Met. Metalloved. **53**, 722 (1982).
[14]V. A. Desnenko, A. S. Panfilov, and A. I. Smirnov, Fiz. Nizk. Temp. **21**, 546 (1995) [Low Temp. Phys. **21**, 424 (1995)].
[15]A. S. Panfilov, Fiz. Nizk. Temp. **41**, 1318 (2015) [Low Temp. Phys. **41**, 1029 (2015)].
[16]E. Fawcett, Phys. Rev. B **2**, 1604 (1970).